Bull Soc Chim Fr (1997) 134, 635-640

Evidence for a macrobicyclic effect on the physico-chemical properties and stability versus pH of imidazolate-bridged dicopper(II) complexes: active centre analogues of Cu_2 superoxide dismutase

Claude Béguin[1]*, Pierre Chautemps[1], Jean-Louis Pierre[1], Eric Saint-Aman[2], Guy Serratrice[1]

[1] *Laboratoire de Chimie Biomimétique, LEDSS UMR CNRS 5616, Université Joseph Fourier;*
[2] *Laboratoire d'Electrochimie Organique et de Photochimie Redox, UMR CNRS D 5630, Université Joseph Fourier, BP 53X, 38041 Grenoble, France*

(Received 14 April 1997; accepted 2 June 1997)

Summary — pH stability and other physico-chemical properties for imidazolate-bridged dicopper(II) complexes of macrocyclic ($\mathbf{L^1}$) and macrobicyclic ($\mathbf{L^2}$) ligands, built with two and three identical subunits respectively, were studied. Electron paramagnetic resonance spectroscopy, UV–visible spectrophotometry and electrochemical studies evidenced a stronger interaction of the imidazolate dicopper entity with the ligand in the case of $\mathbf{L^2}$. The pH stability range (shown both by EPR at 100 K and electronic spectroscopy at room temperature) was larger with $\mathbf{L^2}$ (4.5–12 pH units) than with $\mathbf{L^1}$ (5–9 pH units). The SOD activity (NBT assay) exhibited with both complexes survives to bovine serum albumin for the complex with $\mathbf{L^2}$.

imidazolate-bridged binuclear copper complex / macrobicyclic effect / pH stability / solution spectroscopic study / superoxide dismutase activity

Résumé — Mise en évidence de l'effet macrobicyclique sur les propriétés physico-chimiques et la stabilité en fonction du pH de complexes binucléaires du cuivre (II) : modèles du site actif de la superoxyde dismutase. Sont étudiées la stabilité en pH et d'autres propriétés physico-chimiques de complexes dicuivriques pontés par l'anion imidazolate de ligands macrocycliques ($\mathbf{L^1}$) et macrobicycliques ($\mathbf{L^2}$) construits respectivement à partir de deux ou trois sous-unités identiques. Les spectroscopies de résonance paramagnétique électronique et d'UV–visible ainsi que des études électrochimiques montrent une interaction plus forte de l'entité dicuivrique–imidazolate dans le cas de $\mathbf{L^2}$. Le domaine de stabilité en pH (observé à la fois en RPE à 100 K et en spectroscopie électronique à température ordinaire) est plus grand avec $\mathbf{L^2}$ (4,5–12 unités de pH) qu'avec $\mathbf{L^1}$ (5–9 unités de pH). Les deux complexes montrent une activité SOD (test au NBT) qui se maintient en présence d'albumine de sérum de bœuf seulement avec le complexe $\mathbf{L^2}$.

complexe binucléaire du cuivre à pont imidazole / effet macrobicyclique / stabilité en fonction du pH / étude spectroscopique en solution / activité de la superoxyde dismutase

Introduction

Copper–zinc superoxide dismutase (Cu–Zn SOD) contains in its active site an imidazolate-bridged bimetallic centre [1]. SOD is a catalyst for superoxide (O_2^-) disproportionation [2] and is known to protect cells from its toxic effects. The copper and zinc ions can be removed from the enzyme and substituted by other metals; the dicopper derivative (Cu–Cu SOD) exhibits the same catalytic activity as the native enzyme [3]. Hence, as has been emphasized, imidazolate-bridged dicopper complexes may be considered as good functional models of superoxide dismutase [3]. Several imidazolate-bridged dicopper(II) complexes have been described [3–17], some of which employ a macrocyclic ligand to enhance the solution stability of the complex.

This paper describes the preparation and solution studies (with special emphasis on the determination of the pH range over which the imidazolate bridge is stable) of the imidazolate-bridged dicopper complexes with the macrocyclic $\mathbf{L^1}$ and the macrobicyclic ligand $\mathbf{L^2}$ (fig 1).

The ligands were designed to contain secondary amine groups, owing to their lower sensitivity to hydrolysis (especially at low pH) than imine groups. Imine-containing ligands are used for most of the imidazolate-bridged dicopper(II) complexes described in the literature [3]. We have previously described the complex $[(Cu(im)Cu)\mathbf{L^2}](ClO_4)_3$ [18]. The macrobicyclic ligand $\mathbf{L^2}$ is the same as the macrocyclic ligand $\mathbf{L^1}$, except for a third bridge identical with the two others, between the two bridge-head tertiary nitrogen atoms. Thus, the two ligands are well suited for studying the macrobi-

* Correspondence and reprints

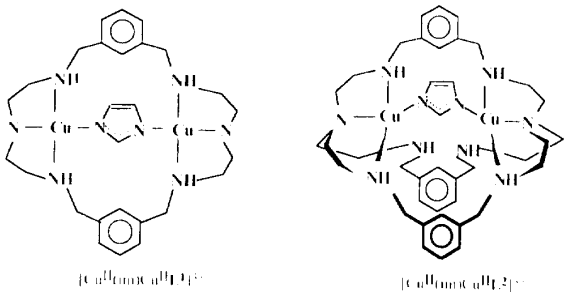

Fig. 1. Formula of $[Cu^{II}(im)Cu^{II}\mathbf{L^1}]^{3+}$ and $[Cu^{II}(im)Cu^{II}\mathbf{L^2}]^{3+}$.

cyclic effect (addition of a third arm to the macrocyclic ligand) [19] on the physico-chemical properties and the SOD activity of the complexes. It is important to determine which structural features are critical for the SOD activity of abiotic models: the two complexes depicted in figure 1 allow comparison of tetra- versus penta-coordination of the copper ions by the same type of ligating groups.

Experimental section: materials and methods

Commercial reagents were used as received without further purification. Solvents were purified by standard methods before use. Elemental analyses were performed by the CNRS Microanalysis Laboratory of Lyon, France.

Spectrometry

EPR spectra were recorded at 100 K on a Bruker ER 100 D spectrometer operating at 9.4 GHz with 2,2-diphenyl-1-picrylhydrazyl as an external calibrant. The pH of the aqueous solution was adjusted before the addition of DMSO to obtain a 1:1 v/v water–DMSO solution prior to cooling to 100 K. UV–visible spectra were obtained on a Perkin-Elmer Lambda 2 spectrophotometer with quartz cells at room temperature. FAB mass spectra in the positive mode were recorded on a Nermag R 1010 C spectrometer equipped with a M-scan (Wallis) atom gun (8 kV, 20 mA).

Electrochemistry

$[(Cu(im)Cu)\mathbf{L^1}](ClO_4)_3$ was studied in aqueous media at pH 7, using a 0.1 mol dm^{-3} KNO_3 solution as supporting electrolyte. Electrochemical experiments were carried out using a PAR model 264-A polarographic analyser, a PAR model 303-A mercury dropping electrode and recorded on a Kipp-Zonen x–y recorder. All experiments were run under an argon atmosphere at room temperature. A standard three-electrode electrochemical cell was used. Potentials are referred to a saturated aqueous calomel reference electrode (SCE). In order to prevent adsorption phenomena at the mercury electrode in aqueous media, the polarograms were recorded in solutions containing a small amount (0.1%) of Triton X100.

Synthesis

$\mathbf{L^1}$ was prepared following the procedure described by Menif et al [20]. The complex $[(Cu(im)Cu)\mathbf{L^1}](ClO_4)_3$ was prepared as follows: a solution of imidazole (680 mg, 10 mmol) in degassed methanol (40 cm^3) was mixed dropwise (30 min) under an argon atmosphere with a methanol solution (100 cm^3) of $Cu(ClO_4)_2$, 6 H_2O (3.7 mg, 10 mmol). The resulting blue solution was stirred for 1 h to give the $[(Cu(im)Cu)](ClO_4)_3$ moiety as described in the literature [14]. Then, 14 cm^3 of the last solution (0.5 mmol of $[(Cu(im)Cu)](ClO_4)_3$) was added dropwise to $\mathbf{L^1}$ (205 mg, 0.5 mmol, in 30 cm^3 of methanol) and the solution was stirred for 3 h. A light-blue precipitate was obtained, washed with cold methanol and dried under vacuum (yield: 74%).

Elemental analysis

Calc for $C_{27}H_{41}N_8Cu_2(ClO_4)_3$ (MW = 902.5): C, 35.9; H, 4.5; N, 12.4; Cu, 14.07; Cl, 11.78.

Found: C, 35.5; H, 4.48; N, 12.17; Cu, 14.03; Cl, 12.10.

FAB$^+$ MS (3-NBA): m/z (1) 803 $[(M - ClO_4)^+]$, m/z (2) 636 $[(M - ClO_4 - Im)^+]$, (1):(2) = 0.7.

The syntheses of the ligand $\mathbf{L^2}$ and the corresponding complex $[(Cu(im)Cu)\mathbf{L^2}](ClO_4)_3$ have been described previously [18, 21].

SOD Assays

Superoxide was generated enzymatically from the hypoxanthine–xanthine oxidase reaction [22]. Superoxide dismutase (SOD) activity was evaluated by the nitroblue tetrazolium (NBT) assay [23] both with and without bovine serum albumin (BSA) added for in vivo type scavenging free cations.

Results and discussion

Preparation of ligands and complexes

- *$[(Cu(im)Cu)\mathbf{L^1}](ClO_4)_3$*

The condensation of isophtalaldehyde with diethylenetriamine in acetonitrile leads to the macrocyclic Schiff base previously described by Menif et al [20]. This tetraimine macrocycle $\mathbf{L'^1}$ (condensation of two isophtalaldehyde and two tris (2-aminoethyl)amine molecules) is not stable. Spontaneously it undergoes a reversible transposition resulting from the intramolecular attack of the imine functions by the secondary amine nitrogen atoms. $\mathbf{L^1}$ was, as usual, obtained from the Schiff base ligand $\mathbf{L'^1}$ upon reduction by NaBH4 in methanol [19, 20]. This reagent displaced the above equilibrium by reactivity on the imine function only. However, we failed to prepare the imidazolate-bridged dicopper(II) complex of $\mathbf{L'^1}$ by using unsuccessfully three different ways: (i) synthesis of the complex $[(Cu(im)Cu)\mathbf{L'^1}]^{3+}$ by using the template effect of the $[(Cu(im)Cu)]^{3+}$ entity prepared according to the literature [13, 14]. This method did not give any cyclisation product; (ii) reaction of the ligand $\mathbf{L'^1}$ with $[(Cu(im)Cu)]^{3+}$ which give only hydrolytic decomposition of this ligand and (iii) reaction of the ligand $\mathbf{L'^1}$ with two copper(II) ions, giving the μ-hydroxo complex as previously described [21], followed by treatment with imidazole. This method leads to hydrolytic cleavage. The complex $[(Cu(im)Cu)\mathbf{L^1}](ClO_4)_3$ was prepared from $\mathbf{L^1}$ and the $[(Cu(im)Cu)]^{3+}$ entity.

• *[(Cu(im)Cu)$\mathbf{L^2}$]$(ClO_4)_3$*

The syntheses of the ligand $\mathbf{L^2}$ and the corresponding complex [(Cu(im)Cu)$\mathbf{L^2}$]$(ClO_4)_3$ have been described previously [18, 21].

Spectroscopy

• *Electron paramagnetic resonance studies*

The anisotropic EPR spectra at 100 K, of dilute solutions of the complexes in water–DMSO (1:1 v/v) glasses, are shown in figure 2.

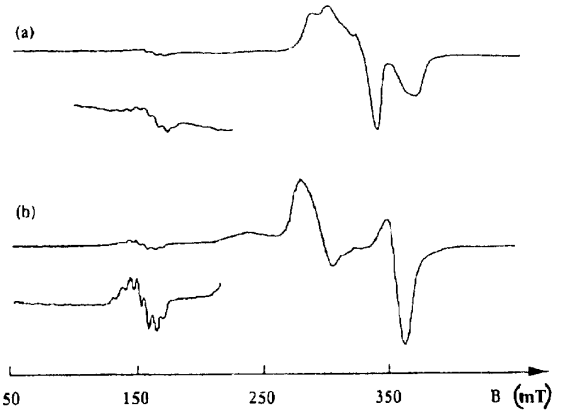

Fig 2. EPR spectra at 100 K in water–DMSO glass. (a): [(Cu(im)Cu)$\mathbf{L^1}$]$(ClO_4)_3$ (1 mmol dm^{-3}); (b): [(Cu(im)Cu)$\mathbf{L^2}$]$(ClO_4)_3$ (1 mmol dm^{-3}).

For the [(Cu(im)Cu)$\mathbf{L^1}$]$(ClO_4)_3$ EPR spectrum, two types of signals are visible in the $\Delta M_s = 1$ and $\Delta M_s = 2$ regions. The latter signal, which lies in the 155 mT range ($g = 4.50$), reveals a spin exchange interaction between the two copper atoms. The signal is comprised of seven lines (relative intensities equal to 1, 2, 3, 4, 3, 2, 1) with a 6.4 mT splitting, which can be attributed to the hyperfine coupling of the electronic spin density with the two copper nuclei with nuclear spin of $I_N = 3/2$. The hyperfine constant of 6.4 mT is approximately half the value found in mononuclear Cu^{II} complexes having the same ligand types and geometry [24], as is expected for homonuclear dimers [25]. The $\Delta M_s = 1$ ($g = 2.11$) region of the spectrum shows two broad signals at 290 and 370 mT assigned to the zero-field splitting interaction with a D value of about 0.058 cm^{-1}. The spectrum is very similar to that of the imidazolate-bridged dicopper complex of a *bis* diene-type ligand [7].

The [(Cu(im)Cu)$\mathbf{L^2}$]$(ClO_4)_3$ EPR spectrum, which has been described previously [18], exhibits a similar $\Delta M_s = 2$ transition (at 161.1 mT, $g = 4.48$) revealing a spin exchange interaction between the two copper ions (seven lines, binomial intensities for two $I_N = 3/2$ nuclei; $A_N = 5.7$ mT). The $\Delta M_s = 1$ ($g = 2.12$) region of the spectrum shows also two broad and two sharper signals respectively at 280 and 400 mT and 280 and 360 mT. These peaks have absorption lineshapes and derivative lineshapes which are attributable to zero-field splitting effects with a D value of 0.070 cm^{-1}[18]. The simulation of the EPR spectra of these two products and of other compounds observed during our studies will be described in detail elsewhere.

• *UV–visible studies*

The spectra of millimolar solutions of the [(Cu(im)Cu)$\mathbf{L^1}$]$(ClO_4)_3$ complex in water or DMSO–water (1:1 v/v) exhibit d–d transitions of copper centered at 630 nm ($\varepsilon = 650$ mol^{-1} dm^3 cm^{-1}) with a shoulder at 550 nm. This indicate two coordinating environments for the two copper ions. The shoulder at 550 nm is related to a square planar geometry. The transition at 630 nm is related to a square pyramidal geometry suggesting the coordination of one water molecule with one of the two copper ions. The 630 nm transition may be compared to that of [Cu(im)Cu(TMDT)$_2$(ClO$_4$)$_2$]ClO$_4$, where TMDT is for 1,1,7,7-tetramethyldiethylenetriamine [26] (with a d–d transition at 624 nm in H_2O–DMSO (1:1 v/v)). This complex, in the solid state, has a square pyramidal structure around each copper atom with four nitrogen atoms lying approximately in the same plane, and a perchlorate oxygen atoms in the apical position. In solution the perchorate anion may be substituted by a water molecule. On the basis of the similar Cu^{II} electronic spectrum the ligand field of [(Cu(im)Cu)$\mathbf{L^1}$]$^{3+}$ should also have similar geometry and strength for one copper.

The spectrum of [(Cu(im)Cu)$\mathbf{L^2}$]$(ClO_4)_3$ in water or water–DMSO solutions displays a broad band (d–d transition) at $\lambda_{max} = 660$ nm ($\varepsilon = 450$ mol^{-1} dm^3 cm^{-1}) with a shoulder at about 750 nm. This can be related to the geometry of the two copper ions intermediate between square pyramidal and trigonal bipyramidal as observed in solid X-ray structure.

Electrochemistry

The electrochemical behavior of [(Cu(im)Cu)$\mathbf{L^1}$]$^{3+}$ and [(Cu(im)Cu)$\mathbf{L^2}$]$^{3+}$ has been studied in an aqueous 0.1 M KNO_3 electrolyte on a mercury dropping electrode (MDE) using an SCE electrode as reference. The voltammetric behavior of [(Cu(im)Cu)$\mathbf{L^1}$]$^{3+}$ is characterized by two cathodic waves at −0.23 V and −1.02 V (fig 3a). Comparison of the intensity of each cathodic wave with that of related electrochemical systems shows that each wave corresponds to two-electron transfer reactions. Thus the first electrochemical wave corresponds to the Cu_2^{II}/Cu_2^{I} redox couple and the second electrochemical wave to the deposition of Cu^0 on the electrode. The two Cu^{II} ions in [(Cu(im)Cu)$\mathbf{L^1}$]$^{3+}$ are reduced at the same potential and the mixed valence [Cu^{II}(im)Cu^{I}] species does not form in detectable amount. Exhaustive electrolysis at −0.4 V on a mercury pool results in the transfer of three electrons per complex molecule. This surprising value suggests that on the time scale of electrolysis, [(Cu(im)Cu)$\mathbf{L^1}$]$^{+}$ slowly decomposes precluding any isolation of the dicuprous complex in relation with the insufficient stabilization of the [Cu^{I}(im)Cu^{I}] entity by $\mathbf{L^1}$.

The electrochemical behavior of [(Cu(im)Cu)$\mathbf{L^2}$]$^{3+}$ appears somewhat different. The cathodic process is characterized by two close waves (fig 3b) at −0.27 V

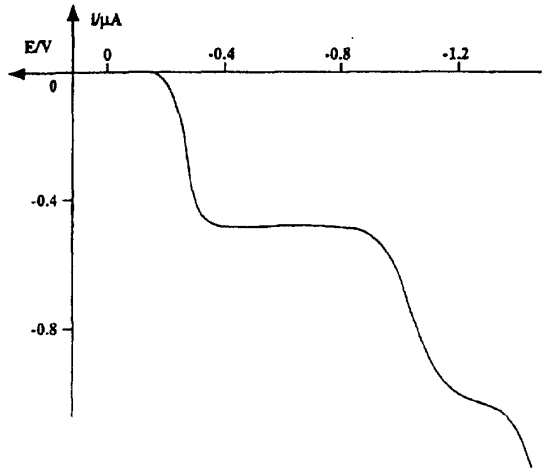

Fig 3a. Polarogram at the mercury drop electrode of $[(Cu(im)Cu)\mathbf{L^1}](ClO_4)_3$ (10^{-4} mol dm^{-3}) in 0.1 mol dm^{-3} KNO_3 aqueous solution at pH = 7.

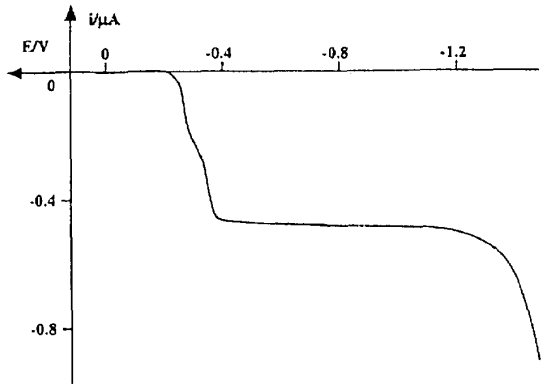

Fig 3b. Polarogram at the mercury drop electrode of $[(Cu(im)Cu)\mathbf{L^2}](ClO_4)_3$ (10^{-4} mol dm^{-3}) in 0.1 mol dm^{-3} KNO_3 aqueous solution at pH = 7.

and −0.34 V, which are assigned to two successive one-electron processes leading respectively to the $[Cu^{II}(im)Cu^{I}\mathbf{L^2}]^{2+}$ mixed-valence complex and to the $[Cu^{I}(im)Cu^{I}\mathbf{L^2}]^{+}$ complex. Like $[(Cu(im)Cu)\mathbf{L^1}]^{3+}$, exhaustive electrolysis is accompanied by the slow decomposition of the reduced species. Further reduction of the complex to the Cu^0 species is not observed before reaching the cathodic limit, due to the reduction of the electrolytic solution.

Although the cathodic process leading to the dicuprous species occurs in the same range of potentials for the complexes with $\mathbf{L^1}$ and $\mathbf{L^2}$, the macrobicyclic structure of $\mathbf{L^2}$ is able to weakly stabilize the mixed-valence $Cu^{II}Cu^{I}$ species by $\leqslant 0.07$ V. This equivalence of the reduction potentials in the Cu_2^{II} complex suggests that, although the Cu^{II} ions interact via an electron spin exchange interaction, the electrostatic interaction of the Cu^{II} ions must be relatively weak in order for each Cu^{II} site not to be perturbated by the redox state of its neighbor. The thermodynamic stability of the $[Cu^{I}(im)Cu^{I}\mathbf{L^2}]^{+}$ complex against further reduction is also enhanced by at least 0.4 V since the Cu^0 species is not formed below −1.4 V, whereas with $\mathbf{L^1}$, Cu^0 deposition is observed at −1.02 V. In addition, with the view of mimicking the SOD activity, the redox processes of these complexes occur in a potential range allowing the disproportionation of the superoxide anion (between −0.4 and +0.65 V).

pH dependent stability of the complexes

The pH dependent stability of both $[(Cu(im)Cu)\mathbf{L^1}](ClO_4)_3$ and $[(Cu(im)Cu)\mathbf{L^2}](ClO_4)_3$ in aqueous solution was studied by EPR and UV–visible spectroscopy.

EPR spectra for $[(Cu(im)Cu)\mathbf{L^1}](ClO_4)_3$ solutions were recorded as a function of pH in frozen water – DMSO (1:1, v/v) solutions at 100 K (fig 4). The stability of the complex is shown by the unchanged spectra in the pH range 5–9.5. At pH $\leqslant$ 4.5, free copper(II) appears in the solution. No intermediate EPR spectrum of the $[(CuCu)\mathbf{L^1}]$ species could be observed. The loss of electronic coupling between the Cu^{II} ions is clearly evidenced by the decrease of the pair of peaks at 280 and 365.5 mT, and from the progressive disappearance of the $\Delta M_s = 2$ transitions at 155 mT. We attribute this decoupling to release of the imidazolate bridge by protonation to form imidazole. At pH $\leqslant$ 4 no more imidazolate bridge is present. At pH = 3 the spectrum exhibits only signals of free Cu^{II} ions in solution suggesting that both imidazolate and amine nitrogen atoms of the ligand are protonated.

The EPR spectra for solutions of $[(Cu(im)Cu)\mathbf{L^2}](ClO_4)_3$ indicate a greater stability of the complex to protonation and release of imidazole. They remain

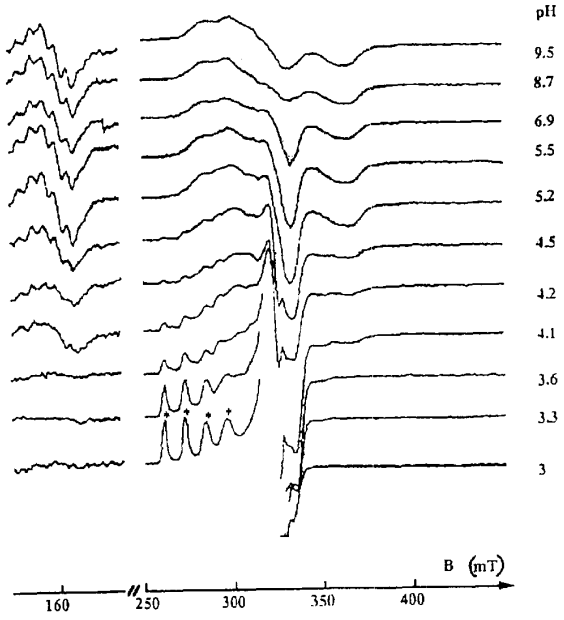

Fig 4. The EPR spectra of $[(Cu(im)Cu)\mathbf{L^1}](ClO_4)_3$ as a function of pH (at 100 K in water–DMSO, 0.002 mol dm^{-3}; (*): free Cu^{2+}).

unchanged in the pH range 4.5–12 (see fig 5 in [18]). The bicyclic ligand clearly enhances the stability of the imidazolate-bridged dicopper unit, especially at high pH, preventing the complex from alkaline hydrolysis.

From UV spectrophotometry, we observed, for $[(Cu(im)Cu)\mathbf{L^1}](ClO_4)_3$, that the d–d transition remained unchanged in the pH range 5–9 (fig 5). At pH < 3.2 the spectrum revealed only free Cu^{II} ions in solution (broad band at 780 nm). At pH > 10, the solution became turbid due to the formation of insoluble hydroxo complexes.

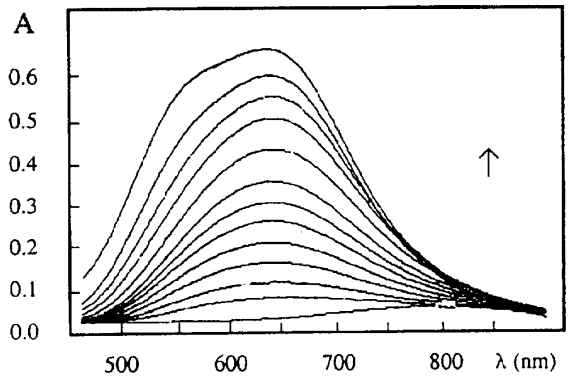

Fig 5. Electronic spectra for $[(Cu(im)Cu)\mathbf{L^1}](ClO_4)_3$ in aqueous solution (0.002 mol dm^{-3}) as a function of pH (pH values: 2.76; 3.28; 3.42; 3.57; 3.60; 3.75; 3.86; 4.02; 4.23; 4.45; 4.66; 5.05; 7.11).

For $[(Cu(im)Cu)\mathbf{L^2}](ClO_4)_3$ (fig 6 in [18]), the same pH stability as that obtained using EPR spectra are observed from UV spectra.

For both $[(Cu(im)Cu)\mathbf{L^1}](ClO_4)_3$ and $[(Cu(im)Cu)\mathbf{L^2}](ClO_4)_3$, the same spectra (both EPR and UV) were obtained upon either increasing as well as decreasing the pH in the same pH range, indicating reversible equilibrium and thus an interesting supramolecular chemistry effect.

SOD assays

$[(Cu(im)Cu)\mathbf{L^1}](ClO_4)_3$ and $[(Cu(im)Cu)\mathbf{L^2}](ClO_4)_3$ exhibit a catalytic activity towards the disproportionation of superoxide anions. The SOD activity exhibited by the former complex does not survive to the addition of bovine serum albumin (BSA) in solution. This implies the capture of copper by albumin (it is well known that the copper complex of albumin does not catalyze the disproportionation of superoxide [2]). The IC_{50} value of 0.5 μmol dm^{-3} determined for $[(Cu(im)Cu)\mathbf{L^2}](ClO_4)_3$, using the nitroblue tetrazolium assay, is higher than the value exhibited by native SOD (0.04 μmol dm^{-3}) and survives to addition of serum albumin, showing that the cryptate structure of $\mathbf{L^2}$ induces a stable environment for the imidazolate-bridged dicopper unit, which is not destroyed by exchange with serum albumin.

Conclusions

$[(Cu(im)Cu)\mathbf{L^1}](ClO_4)_3$ and $[(Cu(im)Cu)\mathbf{L^2}](ClO_4)_3$ provide good models of the active site in Cu_2 SOD. The two complexes exhibit several features in common with the modified enzyme: EPR and electronic spectral parameters are close to those of the protein [27]. Electrochemical studies indicate a quasi-reversible process in the first step of the reduction, as is also the case for the protein [28]. The reduction potentials are significantly lower than for the protein [29]. Nevertheless, the disproportionation of superoxide remains thermodynamically allowed.

$[(Cu(im)Cu)\mathbf{L^1}](ClO_4)_3$ which employs a macrocyclic ligand exhibits a pH range stability for the imidazolate bridge of the same order of magnitude of the abiotic models described in literature (pH from 6 to 10 for the best model described by Lippard et al [26]. The $\mathbf{L^1}$ ligand in $[(Cu(im)Cu)\mathbf{L^1}]$ contains a pair of hydrophobic aromatic arms which create a bidentate chelating ligand capable of forming stable dicopper complexes over a limited pH range in aqueous media. The stability constant for binding of the pair of Cu^{II} ions is assumed to increase relative to the mononuclear complex $[(Cu^{II}(imH))\mathbf{L^1}]$, in which Cu^{II} is replaced by a proton on the imidazolate bridge. The macrobicyclic ligand $\mathbf{L^2}$ enhances the stability of the complex $[(Cu(im)Cu)\mathbf{L^2}]$ to acid- and base-induced dissociation of copper (enhancement of 3.5 units of pH, ie, about 20 kJ mol^{-1} relative to $[(Cu(im)Cu)\mathbf{L^1}]$). We attribute this to the expulsion of solvent from the coordination environment of the former complex, creating a more rigid and hydrophobic environment for the Cu^{II} ions.

Therefore, comparison between $[(Cu(im)Cu)\mathbf{L^1}](ClO_4)_3$ and $[(Cu(im)Cu)\mathbf{L^2}](ClO_4)_3$ clearly evidences the main features of the *macrobicyclic effect*: stabilization of the Cu(im)Cu entity is better with $\mathbf{L^2}$ than with $\mathbf{L^1}$. It is the case for the $[Cu^{I}(im)Cu^{I}]$ entity using electrochemical methods. Stability for $[(Cu^{II}(im)Cu^{II})\mathbf{L^2}](ClO_4)_3$ is enhanced by about 20 kJ mol^{-1} relative to the corresponding complex with $\mathbf{L^1}$. This stability has a drastic consequence on the SOD activity. The catalytic activity of $[(Cu(im)Cu)\mathbf{L^1}](ClO_4)_3$ does not survive in BSA due to the release of copper as is also the case for most of the SOD models described in literature, while the activity of $[(Cu(im)Cu)\mathbf{L^2}](ClO_4)_3$ is unaffected by BSA. Hence, the cryptate structure is clearly the most suited to envisage SOD activity in living media. Mechanistic studies are now in progress.

Acknowledgments

This work was supported by a Research Grant awarded by the European Union (Grant EUREKA SODA 437). We are grateful to the Esteve Laboratories (Barcelona, Spain) and Chauvin SA (Montpellier, France) for their financial support and interest in this work. We thank also Charles Dismukes (Princeton University, Invited Professor in our University during April 1997) for fruitful discussions.

References

1 Tainer J, Getzoff ED, Richardson DC, *Nature* (1983) 306, 284

2 Fridovich I, *Ann Rev Biochem* (1975) 44, 147

3 Strothkamp KG, Lippard SJ, *Acc Chem Res* (1982) 15, 318

4 Gartner A, Weser U, *Topics in Current Chemistry* (1986) 132, 1

5 Weser U, Schubotz LM, Lengfelder E, *J Mol Catal* (1981) 13, 249

6 Coughlin PK, Martin AE, Dewan JC, Watanabe E, Bulkowski JE JM, Lippard SJ, *Inorg Chem* (1984) 23, 1004

7 Coughlin PK, Lippard SJ, *Inorg Chem* (1984) 23, 1446

8 Drew MGB, Cairns C, Lavery A, Nelson SM, *J Chem Soc Chem Commun* (1980), 1122

9 Drew MGB, Mac-Cann M, Nelson SM, *J Chem Soc Dalton Trans* (1981), 1868

10 Drew MGB, Nelson SM, Reedijk J, *Inorg Chim Acta* (1982) 64, L 189

11 Sato M, Ikeda M, Nakaya J, *Inorg Chim Acta* (1984) 93, L 61

12 Cabral JO, Cabral MF, Mac-Cann M, Nelson SM, *Inorg Chim Acta* (1984) 86, L 15

13 Salata CA, Youinou MT, Burrows CJ, *J Am Chem Soc* (1989) 111, 9278

14 Salata CA, Youinou MT, Burrows CJ, *Inorg Chem* (1991) 30, 3454

15 Costes JP, Dahan F, Laurent JP, *Inorg Chem* (1991) 30, 1887

16 Harding CJ, Lu Q, Malone JF, Marss DJ, Martin N, McKee V, Nelson J, *J Chem Soc Dalton Trans* (1995), 1739

17 Mao ZW, Chen MQ, Tan X S, Liu J, Tang WX, *Inorg Chem* (1995) 34, 2889

18 Pierre JL, Chautemps P, Refaif S, Béguin C, El Marzouki A, Serratrice G, Saint-Aman E, Rey P. *J Am Chem Soc* (1995) 117, 1965

19 Lehn JM, *Struct. Bonding* (1973) 16, 1.

20 Menif R, Martell AE, Squattriti PJ, Clearfield A, *Inorg Chem* (1990) 29, 4723

21 Menif R, Reibenspies J, Martell AE, *Inorg Chem* (1991) 30, 3445

22 Fridovich I, in: *CRC Handbook of Methods for Oxygen Radical Research*, Greenwald RA ed, CRC, Boca Raton, 1985, p 51

23 Auclair C, Voisin E, in: *CRC Handbook of Methods for Oxygen Radical Research*, Greenwald RA ed, CRC, Boca Raton, 1985, p 123

24 Chautemps P, Gellon G, Morin B, Pierre JL, Provent C, Refaif S, Béguin CG, El Marzouki A, Serratrice G, Saint-Aman E, *Bull Soc Chim Fr* (1994) 131, 434

25 Wertz JE, Bolton JR, *Electron Spin Resonance Elementary Theory and Practical Applications*, Mc Graw Hill, 2nd edition, 1986

26 O'Young CL, Dewan JC, Lilienthal HR, Lippard SJ, *J Am Chem Soc* (1978) 110, 7291

27 Solomon EI, Penfield KW, Wilcox DE, *Structure and Bonding* (1953) 53

28 a) Banci L, Bertini I, Luchinat C, Piccioli M, *Coord Chem Rev* (1990) 100, 67
b)Sawyer DT, Valentine JS, *Acc Chem Res* (1981) 14, 393

29 Lawrence GD, Sawyer DT, *Biochemistry* (1979) 18, 3045